

*Letter to the Editor***Evidence for inward motion in a galactic cirrus core**

Andreas Heithausen*

Radioastronomisches Institut der Universität Bonn, Auf dem Hügel 71, D-53121 Bonn, Germany (heith@astro.uni-bonn.de)

Received 9 August 1999 / Accepted 24 August 1999

Abstract. Using the IRAM 30 m radiotelescope a dense core in MCLD 123.5+24.9 has been observed in the CS ($J=2\rightarrow 1$), ($3\rightarrow 2$) and ($5\rightarrow 4$) lines. In the lower two rotational lines the cloud extends over $0.03 \text{ pc} \times 0.15 \text{ pc}$ at an adopted distance of 150 pc. The core harbours three dense condensations with full widths at half maximum between 4500 and 6100 AU. Based on C^{18}O observations their masses are estimated to be between 0.06 and $0.12 M_{\odot}$. The southernmost shows asymmetric self-absorbed CS ($2\rightarrow 1$) and ($3\rightarrow 2$) lines with the blue shifted part brighter than the red shifted; the velocity of the ($5\rightarrow 4$) transition is in between the blue and red shifted lines of the lower transitions. These features are well-tested diagnostics of inward motion in molecular clouds. An inward velocity of 4 to 10 m s^{-1} is estimated from the CS lines.

Key words: stars: formation – ISM: kinematics and dynamics – ISM: individual objects: MCLD 123.5+24.9 – ISM: molecules – radio lines: ISM

1. Introduction

High-latitude molecular clouds or galactic cirrus clouds are commonly found to be gravitationally unbound. Their kinematics is largely dominated by turbulence and their virial masses are 1–2 orders of magnitudes larger than their observed masses (Magnani et al. 1987; de Vries et al. 1987; Heithausen 1996). Some of these cirrus clouds harbour dense cores (Mebold et al. 1987) with abundances similar to those dark clouds in star-forming regions (e.g. Großmann et al. 1990). The dense cores found in some cirrus clouds appear to be much closer to virial equilibrium (Großmann & Heithausen 1992) compared to the whole cloud.

It has been found that the star-formation efficiency in high-latitude cirrus clouds must be very low (e.g. Hearty et al. 1999); no low mass T Tauri stars associated with cirrus clouds have been found so far (Martin & Kun 1996). Searches for mm- or submm-sources with low dust temperatures or kinematic signatures of infall motions in galactic cirrus clouds are missing.

Detection of such signatures of beginning star-formation may elucidate the mechanisms that lead to low-mass star-formation.

In this paper I present evidence for inward motion in the dense molecular cloud MCLD 123.5+24.9 located in the Polaris Flare, a huge molecular cirrus cloud in the direction of the north celestial pole (Heithausen & Thaddeus 1990). Its distance is between 130 pc and 240 pc (cf. Heithausen et al. 1993); throughout this paper a distance of 150 pc is adopted. First molecules detected towards MCLD 123.5+24.9 were CO, ^{13}CO , H_2CO , and OH (Großmann et al. 1990), these authors found an increased OH abundance for this cloud. Follow-up observations led to the detection of dense condensations seen in NH_3 , HCO^+ , HCN, and HNC, with abundances consistent with those for dark clouds (Großmann & Heithausen 1992). The kinetic temperature derived from these observations is between 6 K and 15 K. The mass of the core is $1.2 M_{\odot}$ (Großmann & Heithausen 1992, rescaled from 200 pc to 150 pc distance).

2. Observations

The CS ($J=2\rightarrow 1$), ($3\rightarrow 2$), and ($5\rightarrow 4$) transitions have been observed in July 1996 using the IRAM 30 m radio telescope. The beamsizes are $24''$ at 98 GHz, $16''$ at 147 GHz and $10''$ at 245 GHz. Pointing accuracy was better than $3''$. All spectra were obtained with a velocity resolution better than 0.08 km s^{-1} using autocorrelator spectrometers. Maps were obtained with 121 individual positions simultaneously in the three transitions. Spacing between individual positions is $15''$. Because the observations were obtained under average summer conditions the noise level at the higher frequencies especially at the ($5\rightarrow 4$) transition varies significantly. For comparison purpose the C^{18}O ($J=1\rightarrow 0$) data obtained in the key project with the IRAM 30 m telescope (Falgarone et al. 1998) are used. The C^{18}O map covers a much larger area than the CS maps with 2400 individual positions on a 7.5 grid; its angular resolution is $22''$.

3. Results

The CS maps and the C^{18}O map are shown in Fig. 1. The CS core is 0.03 pc wide and extends over 0.15 pc . Three dense condensations are found in the CS ($2\rightarrow 1$) and ($3\rightarrow 2$) maps, labelled CS-A, CS-B, and CS-C. CS-C coincides with the maximum

* Present address: Max-Planck-Institut für Radioastronomie, Auf dem Hügel 69, D-53121 Bonn, Germany

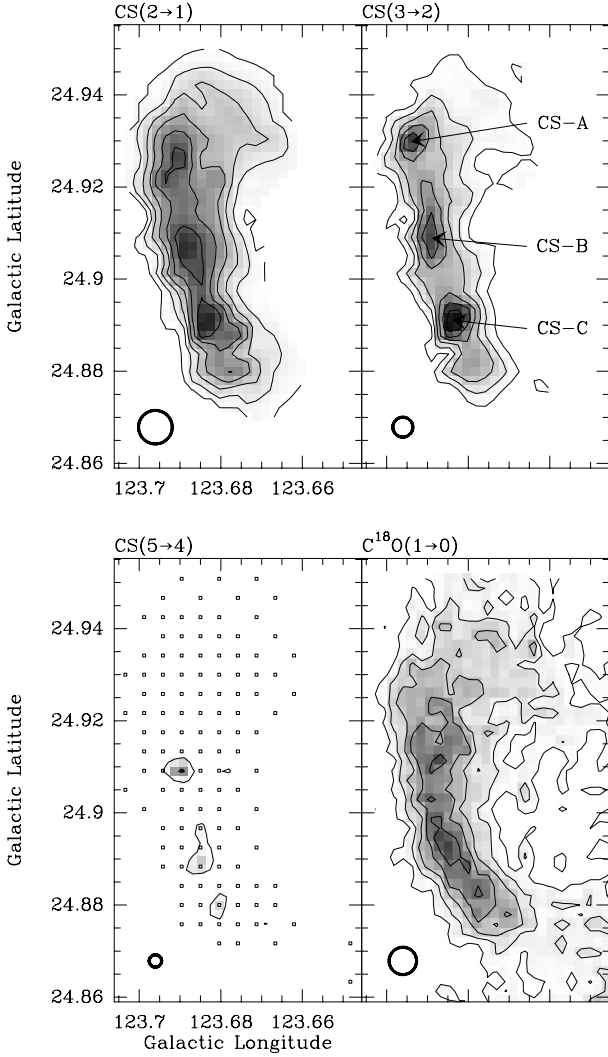


Fig. 1. Total integrated line intensities of the CS (2→1) (top left), (3→2) (top right), and (5→4) transitions (bottom left) and the $C^{18}O$ (1→0) transition (bottom right). Beamsizes are indicated in the lower left corner, observed CS positions are marked in the (5→4) map. Contours are every 0.25 K km s^{-1} starting at 0.25 K km s^{-1} for the CS (2→1) and (3→2) and the $C^{18}O$ (1→0) maps, 0.6 K km s^{-1} starting at 0.6 K km s^{-1} for the CS (5→4) map.

$C^{18}O$ intensity, whereas CS-A and CS-B are not that apparent in the $C^{18}O$ map. Parameters for the three CS lines observed towards the center positions of these dense condensations and the corresponding $C^{18}O$ (1→0) transition are listed in Table 1; the CS spectra of the centre positions are displayed in Fig. 2. The CS (5→4) transition is significantly detected only towards CS-C; towards CS-A and CS-B there is evidence for these lines however with less than the 3σ significance level.

Table 2 summarizes the physical parameters of the three condensations. The full widths at half maximum of the three condensations derived from the CS spectra are 5600 AU, 6100 AU, and 4500 AU for CS-A, CS-B, and CS-C, resp. The masses, estimated from the $C^{18}O$ (1→0) transition adopting an excitation temperature of $T_{\text{ex}} = 5 \text{ K}$ and a $C^{18}O$ abundance of

Table 1. CS and $C^{18}O$ line parameters for the centre positions of the three dense condensations

	CS-A	CS-B	CS-C
CS ($J=2\rightarrow 1$)			
T_{mb}	2.5 (0.3)	2.4 (0.4)	2.14 (0.33) 2.35 (0.33)
v_{LSR}	-4.43 ± 0.01	-4.19 ± 0.02	-4.01 ± 0.02 -4.47 ± 0.02
Δv	0.53 ± 0.02	0.68 ± 0.06	0.26 ± 0.04 0.50 ± 0.06
CS ($J=3\rightarrow 2$)			
T_{mb}	1.81 (0.19)	2.20 (0.36)	1.86 (0.18) 2.69 (0.18)
v_{LSR}	-4.48 ± 0.01	-4.14 ± 0.02	-4.02 ± 0.01 -4.46 ± 0.01
Δv	0.50 ± 0.03	0.58 ± 0.06	0.26 ± 0.04 0.33 ± 0.03
CS ($J=5\rightarrow 4$)			
T_{mb}	[1.3 (0.5)]	[3.0 (1.4)]	2.0 (0.6)
v_{LSR}	$[-4.36 \pm 0.04]$	$[-4.17 \pm 0.06]$	-4.16 ± 0.03
Δv	$[0.27 \pm 0.11]$	$[0.36 \pm 0.12]$	0.29 ± 0.07
$C^{18}O$ ($J=1\rightarrow 0$)			
T_{mb}	3.6 (0.5)	3.0 (0.5)	3.1 (0.6)
v_{LSR}	-4.56 ± 0.01	-4.30 ± 0.02	-4.33 ± 0.03
Δv	0.31 ± 0.04	0.62 ± 0.04	0.61 ± 0.05

Remarks: Parameters are derived from a gaussian fit to the data, those for the lower CS transitions of CS-C adopt 2 components. Units for T_{mb} are (K) and for v_{LSR} and Δv are (km s^{-1}). The CS (5→4) transition is detected only towards CS-C with more than 3σ , there is however indication for this line towards CS-A and CS-B on a lower significance level, the values derived from a formal gaussian fit towards these two positions are therefore listed in square brackets.

Table 2. Physical parameters for the three condensations

	CS-A	CS-B	CS-C
l	123.°694	123.°689	123.°685
b	24.°926	24.°909	24.°892
$FWHM$ (AU)	5600	6100	4500
Mass (M_{\odot})	0.06	0.12	0.07
Density (cm^{-3})	0.8×10^5	1.0×10^5	1.6×10^5
Infall velocity (km s^{-1})	–	–	0.004–0.01

Remarks: Adopted distance 150 pc.

$N(C^{18}O)/N(H_2) = 1.6 \times 10^{-7}$, are between $0.06 M_{\odot}$ and $0.12 M_{\odot}$ for the three condensations. Their virial masses are about $0.2 M_{\odot}$; given the uncertainties in deriving these quantities it is not unreasonable to assume that they are really gravitationally bound. The H_2 volume densities of about 10^5 cm^{-3} are derived by adopting the extent of the clumps to be the same in all three dimensions. These densities are of the same order as the critical density for the CS (3→2) transition.

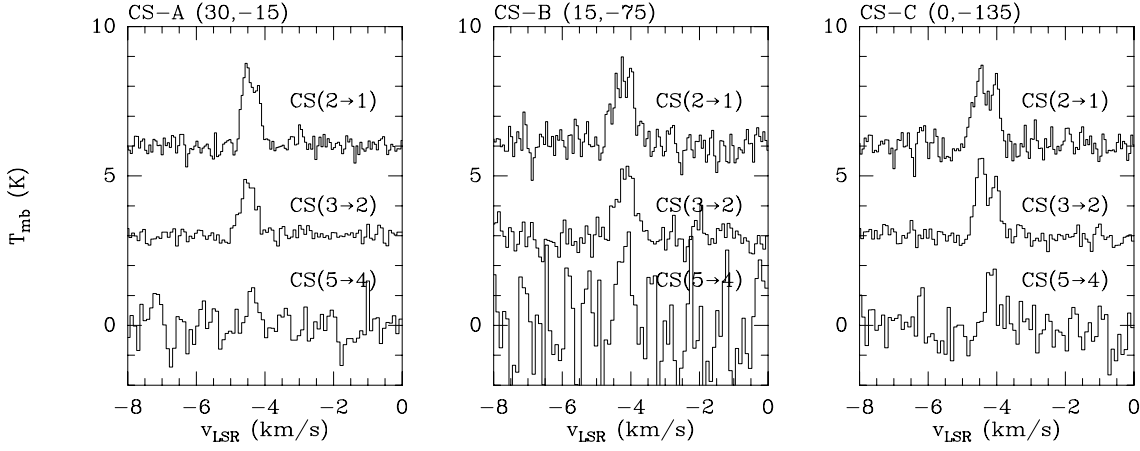


Fig. 2. CS ($J=2\rightarrow 1$), ($3\rightarrow 2$), and ($5\rightarrow 4$) spectra towards the centre positions of CS-A, CS-B, and CS-C. Positions are offsets in arcsec relative to $(l, b) = (123.^\circ 685, 24.^\circ 93)$. For displaying purpose the ($2\rightarrow 1$) spectra have been shifted in the temperature scale by 6 K and the ($3\rightarrow 2$) spectra by 3 K.

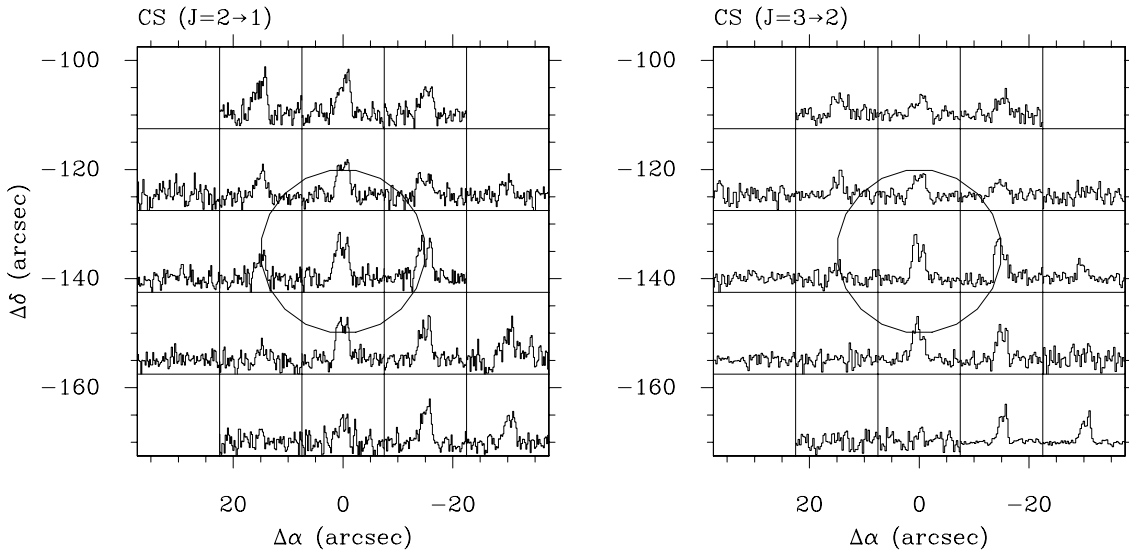


Fig. 3. CS ($J=2\rightarrow 1$) and ($3\rightarrow 2$) spectra towards CS-C. Positions are offsets in arcsec relative to $(l, b) = (123.^\circ 685, 24.^\circ 93)$. The temperature scale is $-0.8 \leq T_{\text{mb}} \leq 4$ K for both maps; velocity scale is $-6.5 \leq v_{\text{LSR}} \leq -2$ km s $^{-1}$. The circles mark the position and size (FWHM) of CS-C.

The spectra towards CS-A and CS-B are well described by single gaussian lines. The spectra towards CS-C are clearly double-peaked in the CS ($2\rightarrow 1$) and ($3\rightarrow 2$) lines with the red shifted peak less intense than the blue shifted peak and only single peaked in the CS ($5\rightarrow 4$) line. Double-peaked ($3\rightarrow 2$) and ($2\rightarrow 1$) lines are only detected towards the immediate surrounding of CS-C (see Fig. 3).

4. Discussion

The CS ($2\rightarrow 1$) and ($3\rightarrow 2$) spectra towards CS-C exhibit the classical double-peaked asymmetric spectral signature of inward motion (see e.g. Zhou 1992; Myers et al. 1996). Before discussing the implications of the discovery it is necessary to exclude other causes for the line shapes. In principle, the line profile can be caused by an unrelated cold absorption layer right in

front of CS-C as discussed e.g. in the case of IRAS 162193–2422 (Menten et al. 1987). Because the number of dense cores in a cirrus cloud is low and the double-peaked lines are only found towards CS-C it is however very unlikely that we observe two unrelated dense cores right on the same line of sight. The velocity of the optically thin C 18 O ($1\rightarrow 0$) line and the CS ($5\rightarrow 4$) line, which is in between the two peaks of the lower transitions, is further proof for that. The most likely explanation is thus that the CS ($2\rightarrow 1$) and ($3\rightarrow 2$) lines are self-absorbed and thus double-peaked, and the ($5\rightarrow 4$) line is single-peaked due to its low optical depth.

The fact that the self-absorption is spatially concentrated on CS-C suggests that the core is centrally condensed as expected for a bound object. We are thus possibly observing the contraction of a part of MCLD 123.5+24.9. To estimate the inward speed of the gas I make use of the simple two-

layer model presented by Myers et al. (1996). This model assumes two uniform regions of equal temperature and velocity dispersion, σ , which are the front and rear halves of a centrally condensed cloud contracting with an inward velocity, v_{in} . In this model, v_{in} can be derived from the observed line profile. I assume that σ is that of the CS (5→4) transition $\sigma = \Delta v / 2.355 = 0.12 \text{ km s}^{-1}$. The inward velocity is then estimated to be between $v_{\text{in}} = 0.004 \text{ km s}^{-1}$ and 0.010 km s^{-1} for the (2→1) and the (3→2) transition, resp. Due to the much better signal-to-noise ratio of the (3→2) spectra the latter value is more reliable. It is similar low as that found for L 1544 (Tafalla et al. 1998). The mass infall rate can be estimated from $dM/dt = 4\pi r_{\text{in}}^2 m n v_{\text{in}}$ with m being the mean molecular mass and n the observed volume density (Myers et al. 1996). For CS-C $dM/dt \approx 1 \times 10^{-7} M_{\odot} \text{ yr}^{-1}$.

There is now evidence for inward motion in a large number of dense cores in star-forming regions (e.g. Gregersen et al. 1997, Mardones et al. 1997). Class 0 and 1 protostars have mainly been selected as targets for those studies. Only two starless dark core have been described so far with evidence for inward motion (Tafalla et al. 1998; Williams & Myers 1999). Whether or not the three dense condensations in MCLD 123.5+24.9 and especially CS-C are associated with low-temperature compact dust sources is unknown so far. Recently, Bernard et al. (1999) have observed this region in different infrared and submm bands and found dust emission with very low dust temperatures ($T_d \approx 13 \text{ K}$) arising from extended cirrus as well as from a compact source. The angular resolution of their observations ($2'$) is however insufficient to resolve the cloud. Clearly, high-angular resolution studies of the dust continuum are required to resolve this issue.

5. Conclusions

I have presented a multi-transition CS study of a dense core in a galactic cirrus cloud. This core harbours three dense low-mass condensations ($\approx 0.1 M_{\odot}$). The spectra of the southernmost condensation show the double-peaked self-absorbed features which are thought to be characteristics of inward motion in a molecular cloud (e.g. Zhou 1992; Myers et al. 1996). A search for a compact dust source and observations of other CS lines or other high-density tracer at higher angular resolution will help to understand the nature of the motions and allow to model the density structure of this condensation.

If the scenario presented here holds true, the observations indicate that even in gravitationally unbound clouds there can be localized regions where the turbulent motions are small and a gravitationally bound core can form, possibly leading to star formation. The stars that might be born in these dense cores will be very low-mass objects, close to the brown dwarf mass-limit. Systematic searches for compact dust sources and further kinematic evidence for inward motion will also shed light on the time-scales and on the mechanisms that lead to the onset of low-mass star-formation.

Acknowledgements. I thank Volkmar Großmann for help during the observations, and Carsten Kramer for critically reading the manuscript.

References

- Bernard J.P., Abergel A., Ristorcelli I. et al. 1999, A&A 347, 640
 de Vries H.W., Heithausen A., Thaddeus P. 1987, ApJ 319, 723
 Falgarone E., Panis J.F., Heithausen A., Perault M., Stutzki J., Puget J.-L., Bensch F., 1998, A&A 331, 669
 Gregersen E.M., Evans N.J., Zhou S., Choi M., 1997, ApJ 484, 256
 Großmann V., Heithausen A., Meyerdierks H., Mebold U., 1990, A&A 240, 400
 Großmann V., Heithausen A. 1992, A&A 264, 195
 Hearty T., Magnani L., Caillault J.P., Neuhäuser R., Schmitt J.H.M.M., Stauffer J., 1999, A&A 341, 163
 Heithausen A., Thaddeus P., 1990, ApJ 353, L49
 Heithausen A., Stacy J.G., de Vries H.W., Mebold U., Thaddeus P., 1993, A&A 268, 265
 Heithausen A., 1996, A&A 314, 251
 Magnani L., Blitz L., Mundy L., 1987, ApJ 295, 402
 Mardones D., Myers P.C., Tafalla M., Wilner D.J., Bachiller R., Garay G., 1997, ApJ 489, 719
 Martin E.L., Kun M., 1996, A&AS 116, 467
 Mebold U., Heithausen A., Reif K., 1987, A&A 180, 213
 Menten K.M., Serabyn E., Güsten R., Wilson T.L., 1987, A&A 177, L57
 Myers P.C., Mardones D., Tafalla M., Williams J.P., Wilner D.J., 1996, ApJ 465, L133
 Tafalla M., Mardones D., Myers P.C., Caselli P. Bachiller R., Benson P.J., 1998, ApJ 504, 900
 Williams J.P., Myers P.C., 1999, ApJ 518, L37
 Zhou S., 1992, ApJ 394, 204